JOURNAL OF MATERIALS SCIENCE 32 (1997) 1665–1670

The effect of Cr_2O_3 additive on the electrical properties of ZnO varistor

YONG HYUK KIM
Department of Electrical Engineering, Kyung Won College, Sungnam-shi, Kyunggi-do, Korea

H. KAWAMURA, M. NAWATA
Department of Electrical and Electronic Engineering, Meijo University, Tempaku-ku, Nagoya 468, Japan

The effect of Cr_2O_3 additive on the leakage conduction and threshold voltage characteristics of bismuth-based ZnO ceramic varistor was studied. The leakage conduction in the voltage range below the threshold voltage increased with increasing Cr_2O_3 concentration and is attributed to the Schottky barrier height. It was found that the increases in the apparent threshold voltage were associated with the lowered donor concentration in the depletion region of the ZnO grain. These results were obtained by measuring *C–V* characteristics, the breakdown voltage at the current density of 10^{-3} A cm^{-2} and the microstructure of ZnO ceramics.

1. Introduction

ZnO ceramic varistors are widely used as components which protect against voltage surge. Its electrical properties can be interpreted in terms of microstructure and grain to rise conduction procedure. The sintering process produces a structure consisting of conductive ZnO grains and grain boundaries which are surrounded by a thin insulating layer [1]. The composition of ZnO ceramic varistors is then directly related to the bulk characteristics and electrical behaviour with non-ohmic properties [2].

So far, oxides of metals such as bismuth, cobalt, manganese, antimony and chromium, have been used as additives to produce ZnO ceramic varistors. They are invariably present in the composition necessary for highly non-ohmic behaviour in ZnO ceramics [3, 4]. Therefore, it is important to investigate the properties of the additives in ZnO ceramics in order to improve the electrical and other microstructure-related characteristics of ZnO varistors. Typical roles of additives are classified into three categories in terms of electrical and physical properties [5, 6]: (1) additives forming the basic microstructure such as Bi_2O_3 and Pr_6O_{11}; (2) additives which improve the non-ohmic properties, such as Co_2O_3 and MnO_2; (3) additives used to improve the reliability, such as Sb_2O_3, TiO_2, Cr_2O_3 and glass. Many studies have been performed on the role of the various additives in relation to non-ohmic properties and microstructure, and they have often been considered for multicomponent systems [7, 8]. Chromium oxide is usually added to react with ZnO and other additives and plays an important role in the electrical behaviour. However, the specific role of chromium oxide as an additive has yet to be established with certainty. Some studies on the microstructure properties related to chromium oxide additive have been published. Maksuoka [9] reported that chromium oxide has a large effect on the phase formation and microstructure in ZnO ceramics, it dissolves uniformly in the ZnO grain and segregates at grain boundaries when ZnO ceramic is sintered below 1450 °C. On the other hand, Inada [10] reported that from X-ray image analysis, the bismuth-rich phase containing the chromium oxide is observed only at a comparatively wide grain boundary and chromium oxide plays an important role in forming the spinel particles which dissolve in it. However, there have been no studies on the effect of chromium oxide additive on the electrical properties.

In the present work, the effect of chromium oxide additive on the leakage conduction and threshold voltage of the ZnO varistor was studied, because leakage current and threshold voltage are important electrical parameters that are necessary for quantitative evaluation of the rated varistor voltage.

2. Experimental procedure

2.1. Preparation of samples

The composition of the varistor powder used in this study was $(98.3 - x)ZnO + 0.7Bi_2O_3 + 0.5\,MnO_2 + 0.5Co_2O_3 + xCr_2O_3$ (mol %), where x varied from 0–1 mol %. All mixtures were ball milled with 0.5 wt % PVA binder for 24 h. After being dried and granulated by a 80 mesh sieve, the powders were pressed at a pressure of 1 t cm^{-2} ($\sim 9.8067 \times 10^{-7}$ N m^{-2}). The pressed samples were sintered in an atmosphere of ambient air in the temperature range 1150–1350 °C for 2 h at a rate of 4 °C min^{-1}, and cooled to room temperature. The surfaces of the sintered samples were lapped and finally fired-on silver electrodes were used for the electrical measurement. The dimensions of the samples used for measurements were 6 mm diameter and 0.8 mm thick. For microstructure observation, the polished samples were etched in a solution of 10% HCl and HF for 15 s.

2.2. Measurement of electrical properties

I–V characteristics of the sample were measured by using d.c high-voltage supply in the current range up to 30 mA, an electrometer and a modified curve tracer with 60 Hz to record the breakdown voltage. *C–V* characteristics were measured using an impedence analyser and a low voltage supply at 1 kHz in the voltage range 0–35 V. The microstructure of the samples was observed by scanning electron microscopy. The average grain size of ZnO ceramics was determined by dividing the length of a line by the number of grain boundaries intercepting it. The non-ohmic coefficient was found from

$$\alpha = \mathrm{d}\log(I)/\mathrm{d}\log(V) \tag{1}$$

where V is the voltage across the sample and I is the current flowing through the sample.

3. Results and discussion

3.1. Leakage conduction in the pre-breakdown region

Fig. 1 shows current–voltage characteristics of the varistor samples sintered at 1150 °C and doped at Cr_2O_3 contents varying from 0–1 mol %. In this experiment, a sintering temperature of 1150 °C was found to be most suitable for obtaining a higher non-ohmic coefficient of ZnO varistor. The estimated non-ohmic coefficient was in the range 30–50 for a current density of 10^{-1} A cm^{-2} with increasing Cr_2O_3 content from 0–1.0 mol %. The ohmic characteristics below about 10^{-4} A cm^{-2} soon became non-ohmic in character. In the current region below about 10^{-4} A cm^{-2}, the leakage current increases slightly with increasing Cr_2O_3 content, indicating the donor-like behaviour of this impurity in the wide band-gap semiconductor lattice of ZnO ceramics. In the non-ohmic region above 10^{-4} A cm^{-2}, the breakdown voltage at constant current increased with increasing Cr_2O_3 content. In the ohmic region, the composition, without Cr_2O_3 additive, had a lower leakage current than that without Cr_2O_3. This may suggest that the number of conducting carriers is increased due to the Cr_2O_3 content. As a result, the leakage current will increase with increase in carrier concentration. Leakage conduction at the pre-breakdown region is related to temperature and is likely to originate from changes in the barrier height due to change in the positive charge density in the depletion region of the ZnO grain [11].

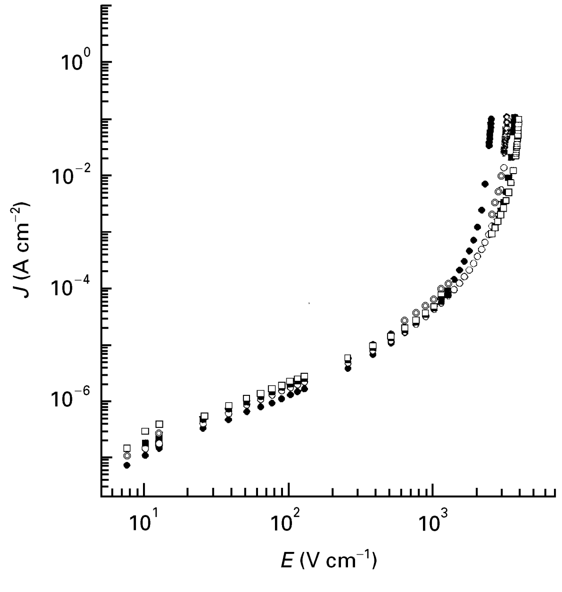

Figure 1 Typical current–voltage characteristics of ZnO varistors at room temperature, measured at different Cr_2O_3 contents: (●) 0, (○) 0.3, (◎) 0.5, (■) 0.7, (□) 1.0 mol %. Sintering temperature 150 °C.

Mahan *et al.* [12] have proposed that at low voltage, tunnelling is improbable and transport is by thermal excitation. Thus, in the pre-breakdown region the current is thermally activated and barrier-height dependent. Hower and Gupta [13] also reported that current–voltage characteristics in the pre-breakdown region are controlled by the Schottky barrier at the grain-boundary layer.

In general, trivalent ions (i.e. Al^{3+} and Cr^{3+}) tend to decrease the resistivity of doped sintered polycrystalline ZnO by supplying extra conduction electrons, and the increased conductivity has been explained in terms of increased concentration of charge carriers [14]. That is, the addition of Cr_2O_3 dopant increases the concentration of conduction electrons and simultaneously reduces the equilibrium concentration of zinc interstitials, so that the increase in electrical conductivity is accompanied by a decrease in the zinc diffusion coefficient. The current at low applied voltage is temperature dependent and expressed by the form

$$J = J_0 \exp(-\phi/kT) \tag{2}$$

where ϕ is the barrier height, k the Boltzmann's constant, T the absolute temperature and J_0 a constant. It is restricted to current values low enough for measurement with negligible Joule heating.

Fig. 2 shows the *I–V* characteristics at various temperatures. The temperature of the samples was varied from 298–413 K. It was observed that the *I–V* curve at the pre-breakdown region has a larger temperature dependence, whereas at the breakdown region it is nearly temperature independent. The variation of the *I–V* curve at the pre-breakdown region may be concerned with the Schottky barrier height [15]. From the temperature of the *I–V* characteristics in the pre-breakdown region in Fig. 2 we can determine the barrier height from the slope of the Arrhenius plot of 1 nJ versus $1/T$. Barrier height exhibits an obvious temperature dependence best described in terms of an activation energy. Fig. 3 shows barrier height as a function of Cr_2O_3 content. The barrier height decreases as the Cr_2O_3 content increases and its value ranged from 0.63–0.57 eV. In this result, it is supposed

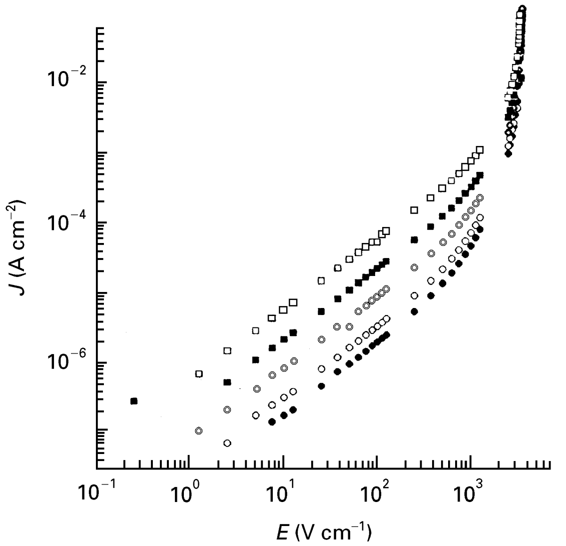

Figure 2 Current–voltage characteristics of ZnO varistors measured at different temperatures: (●) 25 °C, (○) 50 °C, (◎) 80 °C, (■) 110 °C, (□) 140 °C. Sintering temperature 1150 °C, 0.7 mol % Cr_2O_3.

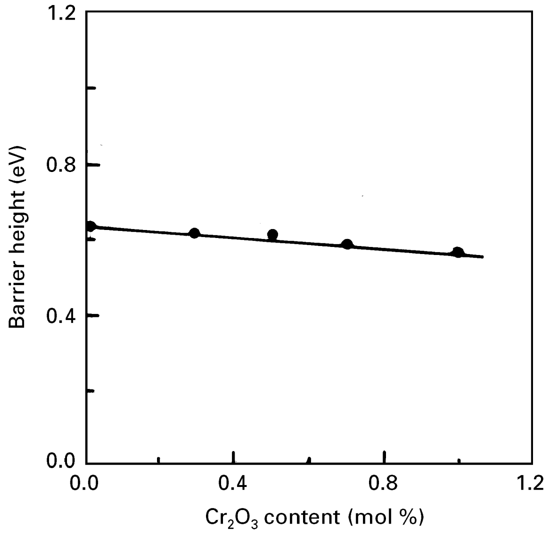

Figure 3 Barrier height of ZnO varistors as a function of Cr_2O_3 content.

that owing to the doped Cr_2O_3, the barrier height decreases so that the increase in leakage current is attributed to the decrease in the barrier height.

3.2. Breakdown conduction and threshold voltage

In order to clearly determine the breakdown characteristics, a variation of the current–voltage trace as a function of Cr_2O_3 content is shown in Fig. 4. *I–V* curves were symmetrical with respect to the applied voltage. Breakdown voltage increases with increasing Cr_2O_3 content. It can be seen that this tendency agrees with the results of *I–V* characteristics in Fig. 1. In the breakdown voltage region, the *I–V* curve trace for a.c. applied voltage is different from that with d.c. applied voltage. In magnitude, the d.c. voltage is higher than the a.c. voltage at 10^{-1} A cm^{-2}. At a critical voltage, the current flow shows an abrupt increase.

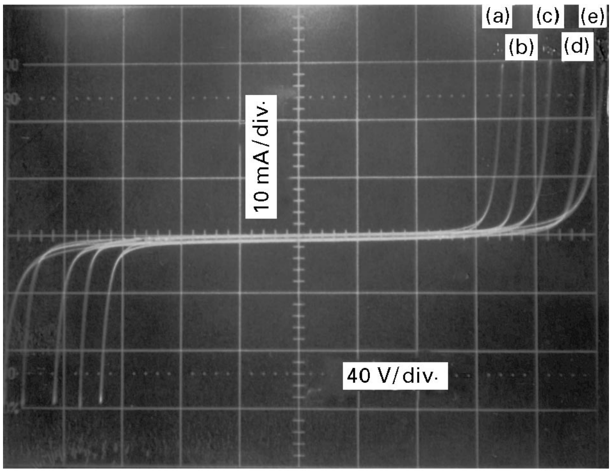

Figure 4 Current–voltage trace of ZnO varistors doped with (a) 0 mol %, (b) 0.3 mol %, (c) 0.5 mol %, (d) 0.7 mol %, (e) 1.0 mol % Cr_2O_3 content.

The critical point of voltage is termed the threshold voltage. It is already known that the threshold voltage is mainly limited by the grain size and the number of barriers. In order to approach a given threshold voltage, variation of grain size and sample thickness were introduced. The macrophic value of threshold voltage of the bulk sample, V_T [16] is

$$V_T = \frac{D}{d} V_t = nV_t \qquad (3)$$

where D and d are the thickness and grain size of the sample, respectively, n is the number of grains in series between the electrodes, and V_t is the breakdown voltage per grain boundary. This implies that threshold voltage is related to the microstructure of the ZnO varistor. Fig. 5 shows the microstructure of samples with various Cr_2O_3 contents. A grain-boundary layer obviously exists, but cannot be clearly observed because the 10% HCl + HF solution etched only the grain boundary without damaging the ZnO grains.

Fig. 6 shows the average grain size as a function of Cr_2O_3 content. The average grain size decreases from 20 μm to 7 μm with increasing Cr_2O_3 content from 0 mol % to 1.0 mol %. Fig. 7 shows the threshold voltage per barrier which was calculated in Fig. 1 and the number of barriers as a function of Cr_2O_3 content. At 10^{-3} A cm^{-2} current density, threshold voltages per barrier were estimated to be in the range 3.75–1.84 V and the number of barriers was in the range 53–100 according to Cr_2O_3 concentration. It also appears that the threshold voltage per barrier decreases with Cr_2O_3 content and the number of barriers increases. In the results, it was found that the product nV_t was not constant, but changes with the Cr_2O_3 content. According to Equation 3, V_t has a dimension effect with voltage per barrier, but the variation of V_t with Cr_2O_3 content suggests that this parameter is an intrinsic property of the grain boundary. Thus it is expected that the apparent threshold voltage V_T will vary with the amount of Cr_2O_3 additive.

Fig. 8 shows the apparent threshold voltage dependence of Cr_2O_3 content. The apparent threshold

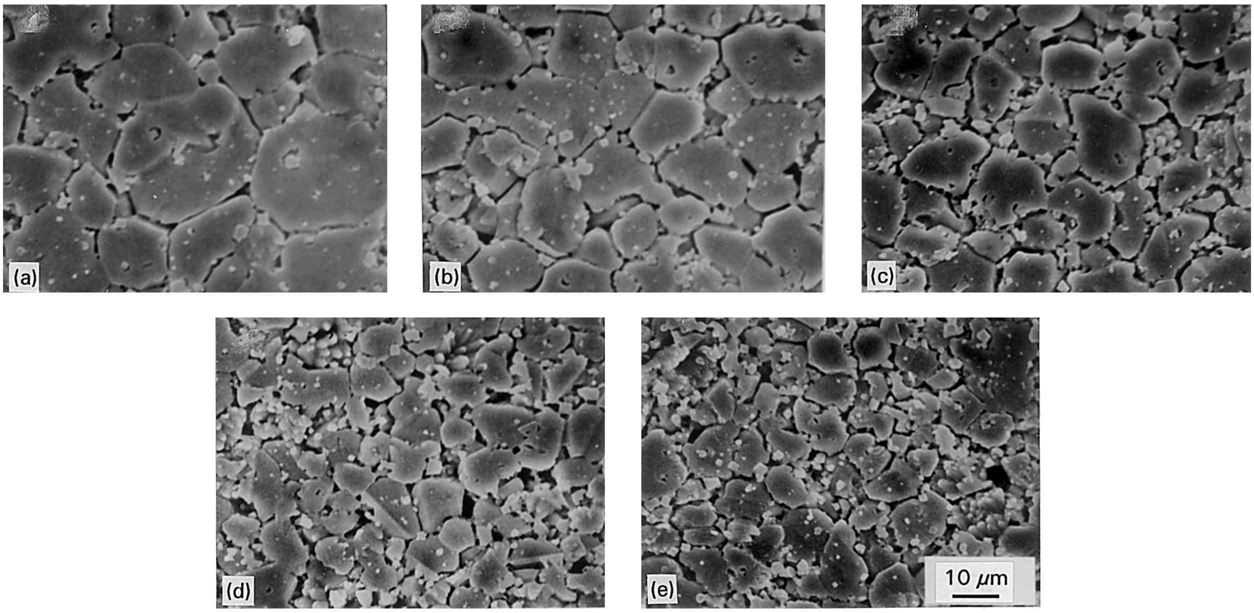

Figure 5 SEM microstructure of ZnO varistors sintered at 1150 °C for 2 h, doped with (a) 0 mol %, (b) 0.3 mol %, (c) 0.5 mol %, (d) 0.7 mol %, (e) 1.0 mol % Cr_2O_3 content.

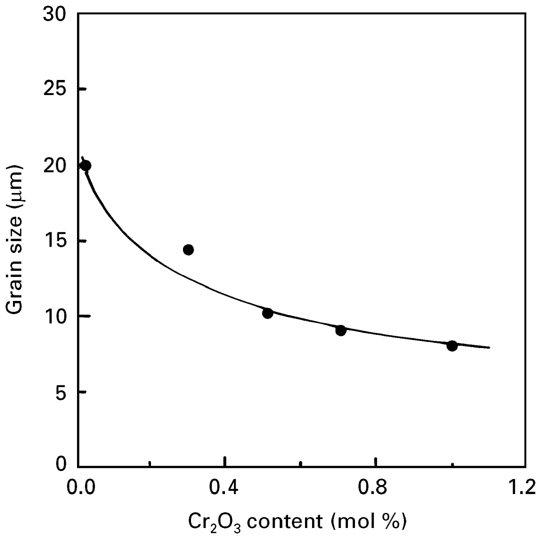

Figure 6 Average grain size of ZnO varistors as a function of Cr_2O_3 content.

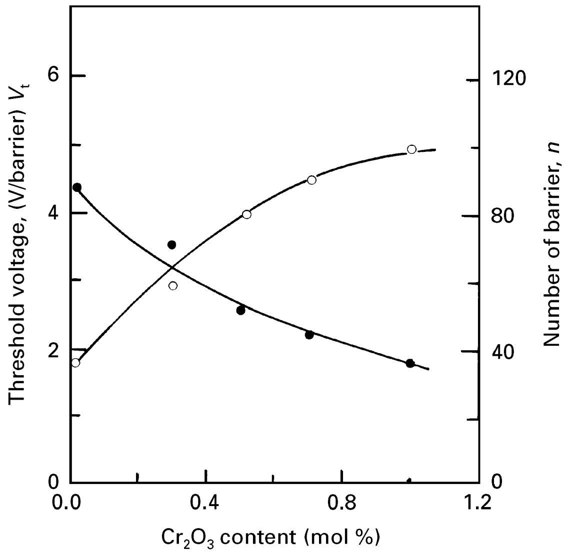

Figure 7 (●) Threshold voltage per barrier and (○) number of barriers of ZnO varistors as a function of Cr_2O_3 content.

voltage increases with Cr_2O_3 concentration and decreases with increasing current density. The apparent threshold voltage, V_T, differs from the threshold voltage per barrier, V_t. That is, V_T increases with increasing Cr_2O_3 content, but V_t decreases. This may be caused by the observed threshold voltage being the sum of series-connected individual barrier threshold voltages, which are dependent upon the direction of electron flow [17]. The mean breakdown voltage per grain in the ceramic is less than that of an isolated grain boundary because there are chains of long grains through the ceramics [18]. It is known that the threshold barrier voltage is strongly dependent on the donor concentration, and the average barrier voltage can be measured in relation to this, which is controlled by doping donors in ZnO ceramics [19]. The capacitance of a ZnO ceramic is mainly attributed to the boundary layer which has a high resistivity. In the samples, the apparent dielectric constant ranges from 3200–2200 at 1 kHz in the presence of Cr_2O_3, which is very much larger than that of ZnO ($\varepsilon_r = 8.5$). The large dielectric constant of the doped Cr_2O_3 additive implies that ZnO grains are good conductors, so that the capacitance is mainly attributed to the grain boundary and the entire voltage is sustained in the grain-boundary layer. Tsuda *et al.* [20] reported that C–V characteristics have been attributed to the change of depletion-layer width at the grain boundary. In order to clarify the behaviour of factors governing these changes, the variation of donor concentration with Cr_2O_3 content was examined by means of capacitance–bias voltage characteristics. Fig. 9 shows the V_t versus $1/C$ plot measured at different Cr_2O_3 contents. It can be seen that $1/C$ increases in proportion with the bias voltage and the effect of Cr_2O_3

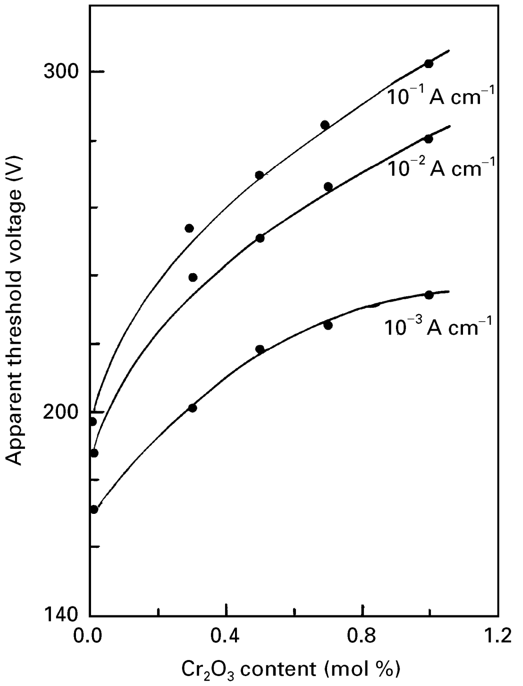

Figure 8 Apparent threshold voltage of ZnO varistors as a function of Cr_2O_3 content.

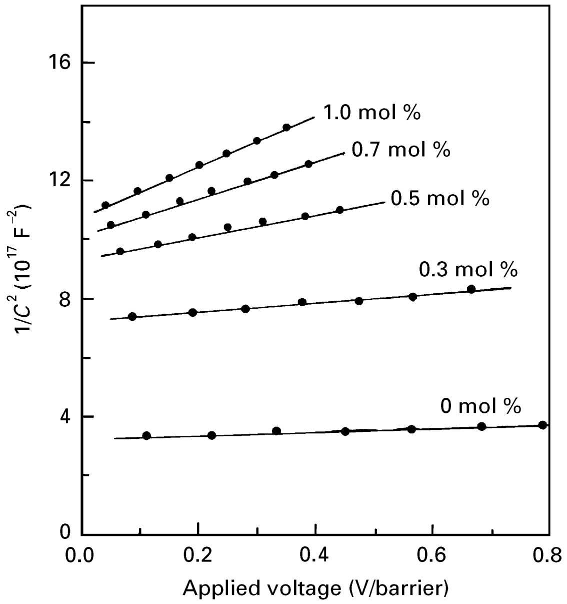

Figure 9 Effect of Cr_2O_3 additive on the voltage dependence of capacitance in a ZnO varistor.

addition has an influence on the slope of the plots. When a voltage is applied to the sample, the double Schottky barrier is deformed and the depletion layer of the biased barrier extends, resulting in a decrease in capacitance. From the slope of the plot in Fig. 9, we can obtain the donor concentration in the ZnO grain. The applied voltage dependence of capacitance for the ZnO varistor can be approximated as [21]

$$N_d = (2n/e\varepsilon\varepsilon_0)[d(V_b)/d(A^2/C^2)] \qquad (4)$$

where ε and ε_0 are the relative dielectric constance of ZnO grain and the permittivity of the free space, respectively, A is the effective electrode area, and n the number of grains in series between the electrodes.

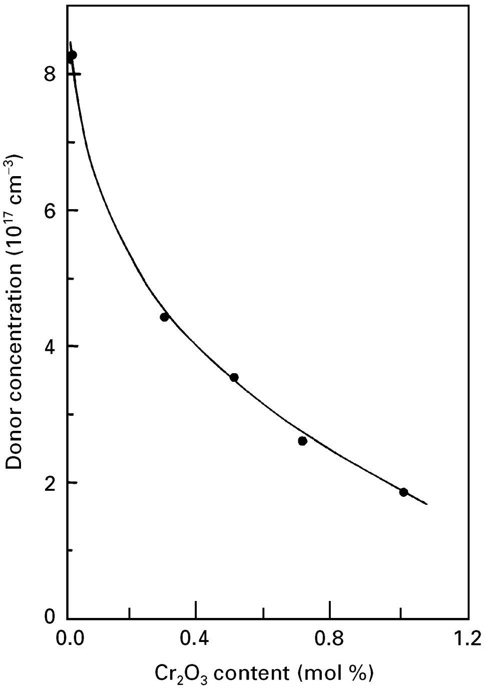

Figure 10 Donor concentration of ZnO varistors as a function of Cr_2O_3 content.

Fig. 10 shows that the donor concentration largely decreases as the Cr_2O_3 additive increases. This is attributed to the fact that as the Cr_2O_3 content is increased the reduction of total capacitance in the grain boundary largely decreases, owing to the reduction of thickness in the insulating grain-boundary barrier by the smaller grain size. Because the Cr_2O_3 behaves as a donor, it oxidizes the interstitial zinc atoms. This oxidation decreases the donor concentration in the grain boundary and should influence the threshold voltage. As can be seen in Fig. 8, the apparent threshold voltage increases from 160 V to 206 V (at 10^{-3} A cm^{-2}) with decrease in donor concentration from 8.3×10^{17} cm^{-3} to 2.0×10^{17} cm^{-3}. Therefore, it can be concluded that the higher threshold voltage of the samples with Cr_2O_3 content is attributed to the remarkable decrease in donor concentration.

4. Conclusions

The effect of Cr_2O_3 additive on the threshold voltage and leakage conduction of bismuth-based ZnO ceramic varistors was investigated by measuring the *I–V* characteristics in the pre-breakdown region, a.c. curves, microstructure, *C–V* characteristics and voltage–temperature dependence. The following conclusions were drawn.

1. Leakage conduction is mainly controlled by the barrier height in the voltage range below the threshold voltage and barrier heights of 0.63–0.57 eV were obtained for the 0–1.0 mol % Cr_2O_3-doped sample.
2. With increasing Cr_2O_3 content, the reduction of the threshold voltage per barrier is caused by the smaller grain size which may contribute to the formation of the thin grain-boundary layer.

3. The increase in the apparent threshold voltage on doping with Cr_2O_3 additive is due to the decrease in donor concentration of the ZnO ceramic which is attributed to the lowered capacitance in the grain-boundary layer.

References

1. Y. C. CHEN and C. Y. SHEN, *J. Appl. Phys.* **69** (1991) 8363.
2. K. EDA, *J. Appl. Phys.* **50** (1979) 4436.
3. D. R. CLARKE, *ibid.* **50** (1979) 6829.
4. J. WONG, *ibid.* **46** (1975) 1653.
5. H. CERVA and W. RUSSWURM, *J. Am. Ceram. Soc.* **71** (1988) 522.
6. B. S. CHIOU and W. JIH, *Br. Ceram. Trans. J.* **85** (1986) 118.
7. E. D. KIM and C. H. KIM, *J. Appl. Phys.* **58** (1985) 3231.
8. U. SCHWING and B. HOFFMANN, *ibid.* **57** (1958) 5372.
9. M. MATSUOKA, *Jpn J. Appl. Phys.* **10** (1971) 736.
10. M. INADA, *ibid.* **17** (1978) 673.
11. K. EDA, A. IGA and M. MATSUOKA, *J. Appl. Phys.* **51** (1980) 2678.
12. G. D. MAHAN, L. M. LEVINSON and H. R. PHILIPP, *ibid.* **50** (1979) 2799.
13. P. L. HOWER and T. K. GUPTA, *ibid.* **50** (1979) 4847.
14. K. HAUFFE, *Z. Phys. Chem.* **196** (1950) 160.
15. Y. SHIN and J. F. CORDARO, *J. Appl. Phys.* **64** (1988) 3994.
16. L. M. LEVINSON and H. R. PHILIPP, *Ceram. Bull.* **65** (1986) 639.
17. E. OLSSON and G. L. DUNLOP, *J. Appl. Phys.* **66** (1989) 3666.
18. P. R. EMTAGE, *ibid.* **50** (1979) 6833.
19. K. MUKAE and I. NAGASAWA, *Adv. Ceram.* **1** (1981) 331.
20. K. TSUDA, K. MUKAE and I. NAGASAWA, *J. Appl. Phys.* **50** (1979) 4475.
21. W. G. MORRIS, *J. Vac. Sci. Technol.* **13** (1976) 926.

Received 14 April 1994
and accepted 13 February 1996